

Magnetism and superconductivity in $\text{Sc}_{5-x}\text{Dy}_x\text{Ir}_4\text{Si}_{10}$ alloys

S. Ramakrishnan, K. Ghosh, and Girish Chandra

Tata Institute of Fundamental Research, Bombay 400 005, India

(Received 26 December 1991)

We report the study of superconductivity and magnetism in $\text{Sc}_{5-x}\text{Dy}_x\text{Ir}_4\text{Si}_{10}$ ($x=0,0.5,1,1.5,2,3,4,4.5,5$) alloys. We find that the superconducting transition temperature decreases as x increases and a linear increase of antiferromagnetic ordering temperature from $x=2$ to 5. We also report an observation of the coexistence of superconductivity and magnetism for $x=1.5$ from resistivity and ac susceptibility measurements in small applied dc magnetic fields.

I. INTRODUCTION

Most of the studies on the coexistence of superconductivity and magnetism are made either on RMO_6S_8 chalcogenides or on RRh_4B_4 borides (R is a rare-earth element).¹ In these systems the superconductivity arises due to Mo clusters and Rh clusters, respectively, while magnetism is due to the rare-earth element. In the case of ternary silicides $\text{Sc}_5\text{Ir}_4\text{Si}_{10}$ (Ref. 2) (where there are no clusters responsible for superconductivity and no direct Ir-Ir contacts), it is of interest to study the effect of the magnetic rare-earth element substitution for Sc on the superconductivity of this system. With this motivation we have studied the effect of Dy substitution for Sc on the normal and superconducting state properties in the $\text{Sc}_5\text{Ir}_4\text{Si}_{10}$ system.

Previous studies³ have shown that the compound $\text{Sc}_5\text{Ir}_4\text{Si}_{10}$ undergoes a superconducting transition (T_C) below 8.5 K whereas $\text{Dy}_5\text{Ir}_4\text{Si}_{10}$ becomes antiferromagnetic (T_N) below 5 K. We have reported detailed susceptibility and resistivity studies on $\text{Dy}_5\text{Ir}_4\text{Si}_{10}$ which exhibits superzone effects near the antiferromagnetic transition.⁴ In this paper we present our detailed study of normal-state resistivity, susceptibility, transition temperature (T_C, T_N) for the $\text{Sc}_{5-x}\text{Dy}_x\text{Ir}_4\text{Si}_{10}$ ($x=0,0.5,1,2,3,3.5,4,4.5,5$) system. We also report the obser-

vation of coexistence of superconductivity and magnetism in the $\text{Sc}_{3.5}\text{Dy}_{1.5}\text{Ir}_4\text{Si}_{10}$ alloy by performing resistivity and ac susceptibility measurements in various dc magnetic fields.

II. EXPERIMENTAL DETAILS

All samples were made by melting the individual constituents in an arc furnace under high-purity argon atmosphere. The purity of Sc, Dy, and Ir is 99.9% while that of Si is 99.999%. All the samples are found to have the tetragonal structure of the type PM 3N ($\text{Sc}_5\text{Co}_4\text{Si}_{10}$ structure). The lattice constants a and c of $\text{Sc}_5\text{Ir}_4\text{Si}_{10}$ and $\text{Dy}_5\text{Ir}_4\text{Si}_{10}$ agree with the previously published data.³ The variation of a and c with concentration x in $\text{Sc}_{5-x}\text{Dy}_x\text{Ir}_4\text{Si}_{10}$ is shown in Fig. 1. The temperature dependence of susceptibility (χ) was measured using a Quantum Design squid magnetometer (in a field of 1 KOe from 2 to 300 K) and a home-built ac susceptometer⁵ (from 300 to 1.5 K in a field of 1 Oe). The resistivity was measured using 4-probe dc technique and the contacts were made using ultrasonic solder (with indium and non-superconducting solder from Oxford Instruments, United Kingdom) on a cylindrical sample of 2 mm diameter and 10 mm length. The temperature was measured using a

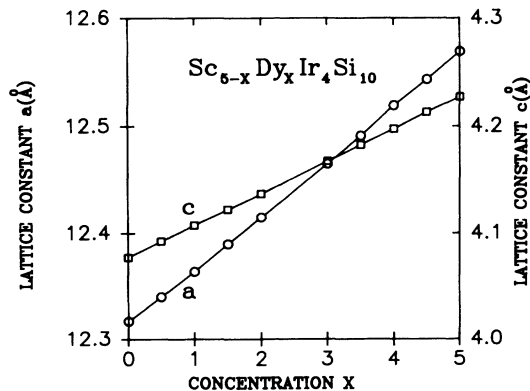


FIG. 1. Variation of lattice constants a and c with concentration x in $\text{Sc}_{5-x}\text{Dy}_x\text{Ir}_4\text{Si}_{10}$.

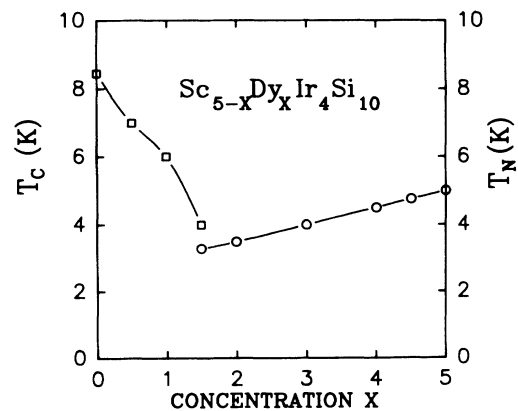


FIG. 2. Dependence of the superconducting transition temperature T_C antiferromagnetic ordering temperature T_N with x in $\text{Sc}_{5-x}\text{Dy}_x\text{Ir}_4\text{Si}_{10}$.

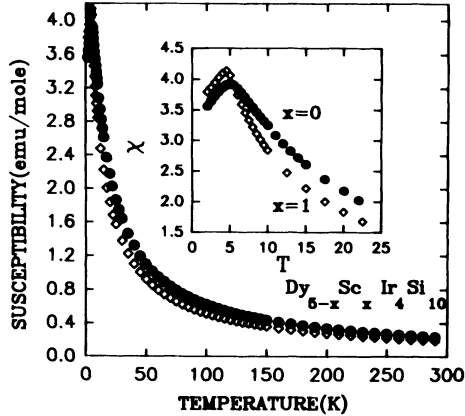


FIG. 3. Variation of $\chi(T)$ of $\text{Dy}_{5-x}\text{Sc}_x\text{Ir}_4\text{Si}_{10}$ for $x=0$ and $x=1$ from 2 to 300 K. The inset shows $\chi(T)$ from 2 to 25 K.

calibrated Si diode (zero-field) and carbon glass (in-field) sensors (Lake Shore, USA). The sample voltage was measured with a Keithley nanovoltmeter with a current of 20 mA using a 20-ppm-stable HP current source. All the data were collected via an IEEE488 interface using a PC/AT machine.

III. RESULTS AND DISCUSSION

A. Susceptibility studies on antiferromagnetic samples ($x \geq 2.0$)

The transition temperature (both T_C and T_N) dependence on the concentration x of Dy is shown in Fig. 2. We find that T_N decreases almost linearly from 5 to 3.5 K as x decreases from 5 to 2. The observed moment (from the high-temperature susceptibility data) is around $10.6\mu_B$ which is the free-ion value for Dy. The temperature dependence of χ of two samples ($\text{Dy}_5\text{Ir}_4\text{Si}_{10}$, $\text{Dy}_4\text{Sc}_1\text{Ir}_4\text{Si}_{10}$) from 2 to 300 K is shown in Fig. 3. The temperature dependence of χ from 2 to 25 K is shown in the inset. One can observe the AF state around 5.0 K for the parent sample and 4.5 K for the Sc substituted one where $d(\chi T)/dT$ shows a maximum. One can also see

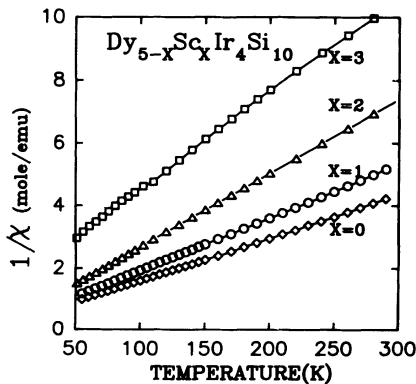


FIG. 4. Plot of $1/\chi(T)$ for $\text{Dy}_{5-x}\text{Sc}_x\text{Ir}_4\text{Si}_{10}$ ($x=0, 2, 3$) with temperature from 50 to 300 K which shows the linear dependence.

TABLE I. Fitted values for the parameters used in Curie-Weiss law for different Dy-rich ($\text{Dy}_{5-x}\text{Sc}_x\text{Ir}_4\text{Si}_{10}$) samples.

Sample	Range	C	Θ_N	T_N	μ_{eff}
$\text{Dy}_5\text{Ir}_4\text{Si}_{10}$	100–300 K	73.8	18.1 K	5.0 K	$10.6\mu_B$
$\text{Dy}_4\text{Sc}_1\text{Ir}_4\text{Si}_{10}$	100–300 K	59.8	15.8 K	4.5 K	$10.6\mu_B$
$\text{Dy}_3\text{Sc}_2\text{Ir}_4\text{Si}_{10}$	100–300 K	42.2	13.0 K	4.0 K	$10.6\mu_B$
$\text{Dy}_2\text{Sc}_3\text{Ir}_4\text{Si}_{10}$	100–300 K	27.6	11.0 K	3.5 K	$10.5\mu_B$

that high-temperature $\chi(100 < T < 300 \text{ K})$ data shows Curie-Weiss law [$\chi(T) = C/(T - \Theta_N)$] from Fig. 4. The other samples show similar dependence and the values of T_N , Θ_N , and μ_{eff} are given in Table I. It will be interesting to study the anisotropy effects in this system using single crystals.

B. Resistivity studies on antiferromagnetic samples ($x \geq 2.0$)

In order to understand the resistivity (ρ) dependence on temperature we have separated the resistivity data into two regions, namely, the low-temperature region ($T \leq \Theta_D/10$) and the high-temperature region (50–300 K)

1. Low temperature resistivity studies ($T_N < T < \Theta_D/10$)

The low-temperature resistivity of the various alloys are shown in Fig. 5. Here we find in the $\text{Dy}_5\text{Ir}_4\text{Si}_{10}$ sample, a broad minimum in ρ around 17 K and a maximum around 6 K. Such a minimum has been seen in many antiferromagnetic rare-earth metals^{6–8} which arises due to magnetic superzone effects. In the case of rare-earth metals like Dy the resistivity shows a minimum followed by a maximum along the c axis before it decreases due to antiferromagnetic ordering.⁸ This has been attributed to the magnetic superzone effect which arises because of the fact that the antiferromagnetic phase has a periodic arrangement along the c axis which is incommensurate with that of the lattice. However, such effects are not reported in

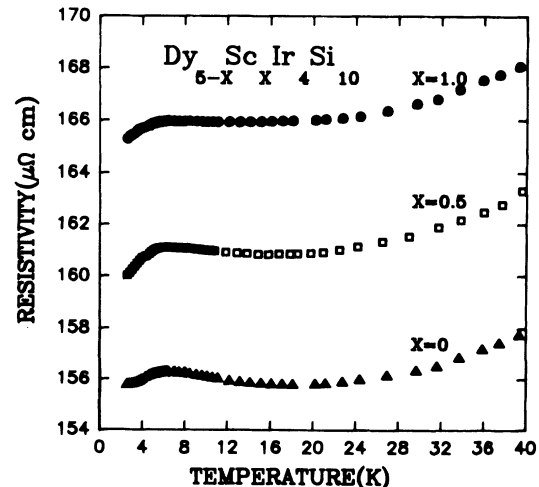


FIG. 5. Temperature dependence of resistivity $\text{Dy}_{5-x}\text{Sc}_x\text{Ir}_4\text{Si}_{10}$ from 2 to 40 K.

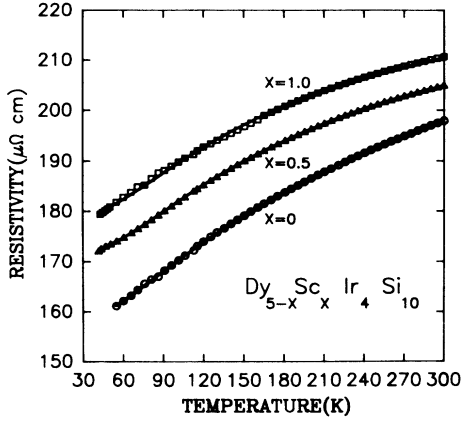


FIG. 6. Temperature dependence of resistivity $\text{Dy}_{5-x}\text{Sc}_x\text{Ir}_4\text{Si}_{10}$ from 50 to 300 K.

intermetallic compounds. Only one paper⁹ has observed this effect in substituted samples and not in an antiferromagnetic compound like $\text{Dy}_5\text{Ir}_4\text{Si}_{10}$.

One can understand the minimum and the maximum in ρ near the antiferromagnetic transition as follows. If one assumes an oscillatory arrangement of $4f$ spins, the conduction electrons will experience a periodic potential through the s - f interaction whose period is incommensurate with that of the crystal lattice. This periodic potential, together with that of the lattice, produces gaps in the energy dispersion of conduction electrons. When the gap appears in the conduction band, the effective number of electrons are reduced. So, near the magnetic transition, this increases the resistivity of the sample. However, spin disorder scattering (due to thermal fluctuations) decreases resistivity as one approaches T_N from room temperature. The combination of these two effects results in the unusual dependence of ρ on temperature along the c axis in many rare-earth elements (Dy, Tm, Er, Eu, Ho, and Gd). The ρ along the a axis shows normal behavior of a magnetic material.

We also see that the minimum becomes shallower as x increases in $\text{Dy}_{5-x}\text{Sc}_x\text{Ir}_4\text{Si}_{10}$ and disappears for $x=2$ and above. Although our samples are polycrystalline we can see the superzone effect clearly in our alloys. However, to compare with theory it is essential to do transport measurements in single crystals of $\text{Dy}_5\text{Ir}_4\text{Si}_{10}$ and its alloys and also the neutron diffraction study to estimate the reduced moment.

2. High-temperature resistivity studies (50 K < T < 300 K)

The high-temperature $\rho(T)$ data for various Dy-rich alloys are shown in Fig. 6. All the alloys show an initial in-

TABLE II. Fitted values for the parameters used in parallel resistor model for different Dy-rich $\text{Dy}_{5-x}\text{Sc}_x\text{Ir}_4\text{Si}_{10}$ samples.

Sample	Range	ρ_0 $\mu\Omega$ cm	C_1	Θ_D K	ρ_{MAX} $\mu\Omega$ cm
$\text{Dy}_5\text{Ir}_4\text{Si}_{10}$	50–300 K	397.0	1150.0	406.2	266.4
$\text{Dy}_{4.5}\text{Sc}_{0.5}\text{Ir}_4\text{Si}_{10}$	50–300 K	555.0	1181.1	315.3	262.0
$\text{Dy}_4\text{Sc}_1\text{Ir}_4\text{Si}_{10}$	50–300 K	521.4	1335.7	309.3	249.9

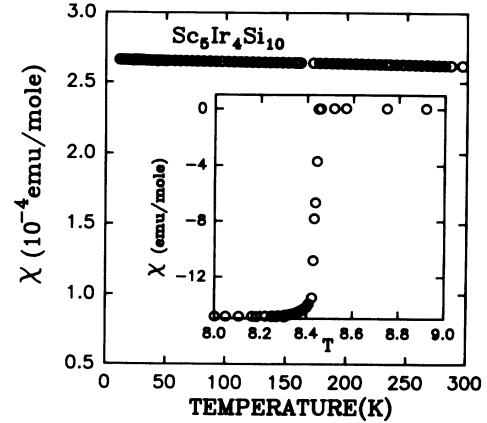


FIG. 7. Temperature dependence of susceptibility of $\text{Sc}_5\text{Ir}_4\text{Si}_{10}$. The inset shows the superconducting transition.

crease in ρ and tendency toward saturation at high temperature. We believe that this saturation has nothing to do with either magnetism or superconductivity in this system. Such a deviation from linear temperature dependence at high temperature has been seen in many alloys where the saturation is attributed to the high value of ρ of these alloys at high temperatures. One of the models which describe the $\rho(T)$ of nonmagnetic materials is known as the parallel resistor model. In this model the expression for $\rho(T)$ is given by

$$\frac{1}{\rho(T)} = \frac{1}{\rho_I(T)} + \frac{1}{\rho_{\text{MAX}}}, \quad (1)$$

where ρ_{MAX} is the saturation resistivity which is independent of temperature and $\rho_I(T)$ is the ideal temperature-dependent resistivity. Further, the ideal resistivity is given by the following expression. The only assumption we have made in addition to the above model is to assume a linear temperature dependence of spin-disorder scattering at high temperature:

$$\rho_I(T) = \rho_0 + C_1(T/\Theta_D)^3 \int_0^{\Theta_D/T} \frac{x^3 dx}{(1-e^{-x})(e^x-1)} + C_2 T, \quad (2)$$

where ρ_0 is the residual resistivity the second term is due

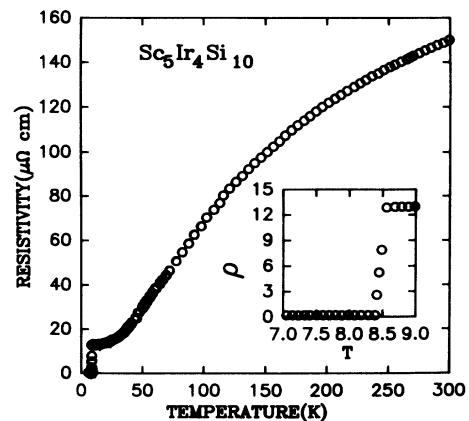


FIG. 8. Temperature dependence of resistivity of $\text{Sc}_x\text{Ir}_4\text{Si}_{10}$. The inset shows the superconducting transition.

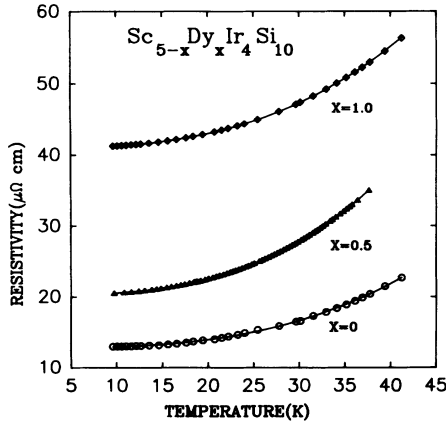


FIG. 9. Low-temperature resistivity of Sc-rich ($\text{Sc}_{5-x}\text{Dy}_x\text{Ir}_4\text{Si}_{10}$) alloys.

to phonon-assisted electron scattering similar to the s - d scattering in transition metal alloys. This model fits fairly well to the data as one can see from Fig. 6 (continuous lines are the fitted values). The values of the various parameters for different alloys are given in Table II. Here one can see that the coefficient C_1 increases as the Sc content increases in these alloys. The value of the ρ_0 is very much larger than the measured resistivity at low temperature. The reason for this behavior is not well understood. Such a discrepancy is noted for many transition metal alloys. A complete analysis over all temperatures requires a detailed transport measurement on single crystals of these samples and crystal-field energy-level scheme of this system.

2. Susceptibility studies on superconducting samples ($x < 2.0$)

The temperature dependence of the susceptibility of $\text{Sc}_5\text{Ir}_4\text{Si}_{10}$ is shown in Fig. 7. The inset shows the superconducting transition of this sample at 8.5 K with the transition width less than 50 mK. The total susceptibility (Pauli spin term and Van Vleck dia- and paramagnetism of ion cores) is positive and shows a very small temperature dependence from 300 to 10 K. This data agrees with the earlier report by Braun and Segrè.³

D. Resistivity studies on superconducting samples ($x < 2.0$)

The temperature dependence of ρ for the $\text{Sc}_5\text{Ir}_4\text{Si}_{10}$ sample is shown in Fig. 8. The inset shows the superconducting transition observed below 8.5 K. The value of

TABLE III. Fitted values for the various parameters used in the power law dependence of resistivity of Sc-rich ($\text{Sc}_{5-x}\text{Dy}_x\text{Ir}_4\text{Si}_{10}$).

Sample	Range	ρ_0 $\mu\Omega \text{ cm}$	A	n	T_C
$\text{Sc}_5\text{Ir}_4\text{Si}_{10}$	10–40 K	12.80	0.000 14	3.0	8.45
$\text{Sc}_{4.5}\text{Dy}_{0.5}\text{Ir}_4\text{Si}_{10}$	10–40 K	20.22	0.000 40	2.9	7.00
$\text{Sc}_4\text{Dy}_1\text{Ir}_4\text{Si}_{10}$	10–40 K	40.95	0.000 46	2.8	6.00

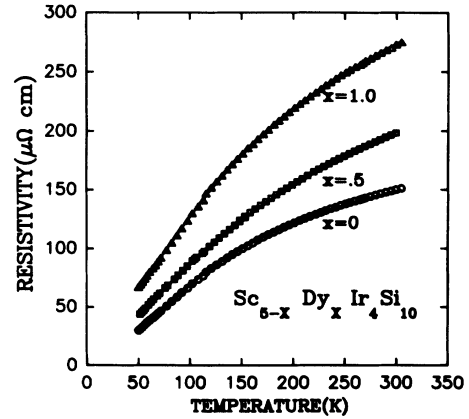


FIG. 10. High-temperature resistivity of Sc-rich ($\text{Sc}_{5-x}\text{Dy}_x\text{Ir}_4\text{Si}_{10}$) alloys.

the resistivity at room temperature is around $150 \mu\Omega \text{ cm}$ which is 10 times less than the previously reported value.¹⁰ Our measurements (rods of dimension $10 \times 2 \text{ mm}^2$ with density 6.81 g/cm^3) on two different samples yielded the same values within 5%. The sharp superconducting transition and no impurities detected in the x-ray analysis show that the samples are of good quality.

1. Low-temperature resistivity ($T < \Theta_D / 10$)

The low-temperature resistivity of Sc-rich alloys is shown in Fig. 9. All the samples show a power-law dependence ($\rho = \rho_0 + T^n$), where the value of n decreases with increasing Dy substitution. For nonmagnetic alloys, one can expect a T^3 term similar to Wilson's model and this power decreases as more magnetic rare-earth atoms are added and for pure magnetic compound one expects a dominance of the T^2 term in the resistivity due to Dy spins ordering at low temperatures. The values of the various parameters used in this fitting are given in Table III.

2. High-temperature resistivity ($50 \text{ K} < T < 300 \text{ K}$)

The high-temperature resistivity data for various Sc-rich alloys are shown in Fig. 10. Here as we have mentioned before, the ρ shows a deviation from linear temperature dependence. According to Allen and co-workers¹¹ such a dependence is expected of high resistance metallic samples because the mean-free path of the electrons is short and they are of the order of interatomic spacing. Hence the classical assumption in the Boltzmann transport equation, namely, $k_F l \gg l$ (where

TABLE IV. Fitted values for the various parameters used in the parallel resistor model for Sc-rich ($\text{Sc}_{5-x}\text{Dy}_x\text{Ir}_4\text{Si}_{10}$).

Sample	Range	ρ_0 $\mu\Omega \text{ cm}$	C_1	Θ_D K	ρ_{max} $\mu\Omega \text{ cm}$
$\text{Sc}_5\text{Ir}_4\text{Si}_{10}$	50–300 K	19.75	1028.9	391.59	241.04
$\text{Sc}_{4.5}\text{Dy}_{0.5}\text{Ir}_4\text{Si}_{10}$	50–300 K	31.53	1106.2	363.3	350.0
$\text{Sc}_4\text{Dy}_1\text{Ir}_4\text{Si}_{10}$	50–300 K	53.40	1282.6	356.9	534.9

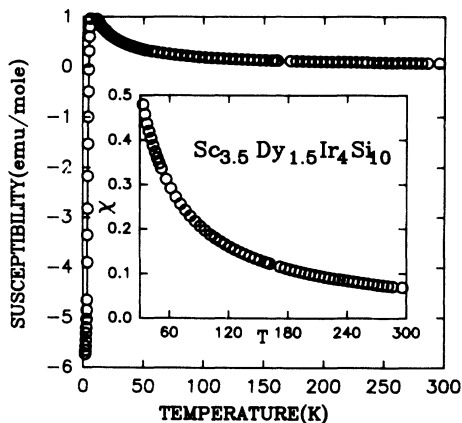


FIG. 11. Temperature dependence of susceptibility of $\text{Sc}_{3.5}\text{Dy}_{1.5}\text{Ir}_4\text{Si}_{10}$. The inset shows the temperature dependence of χ from 60 to 300 K.

k_F is the Fermi wave vector, l is the mean-free path), is no longer valid in these compounds. They suggest that the parallel resistor model [Eq. (2) without the linear term] is appropriate for these systems. We fitted the resistivity data for Sc-rich alloys using this model and the fitted values are shown by the continuous lines in Fig. 10. The values of the various parameters used in this model are given in Table IV. The value of the Θ_D obtained from this analysis agrees very well with the heat capacity results¹² for the $\text{Sc}_3\text{Ir}_4\text{Si}_{10}$ sample. This gives the necessary credibility to this model. One also finds that both ρ_0 , C_1 , and ρ_{\max} increase with Dy substitution. On the other hand, Θ_D decreases with increasing Dy in these alloys.

E. Coexistence of superconductivity and magnetism in $\text{Sc}_{3.5}\text{Dy}_{1.5}\text{Ir}_4\text{Si}_{10}$

1. Resistivity and susceptibility studies

The temperature dependence of the susceptibility (χ) of this sample is shown in Fig. 11. The inset shows the tem-

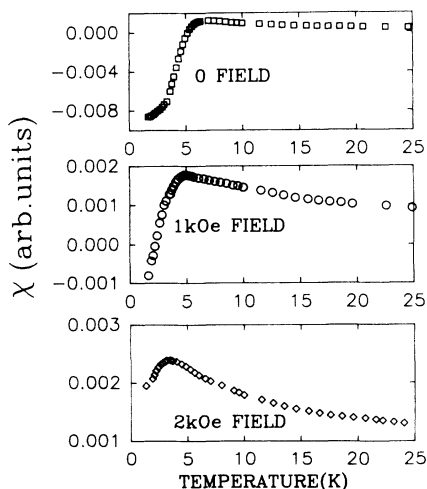


FIG. 12. Ac susceptibility of $\text{Sc}_{3.5}\text{Dy}_{1.5}\text{Ir}_4\text{Si}_{10}$ in dc magnetic fields.

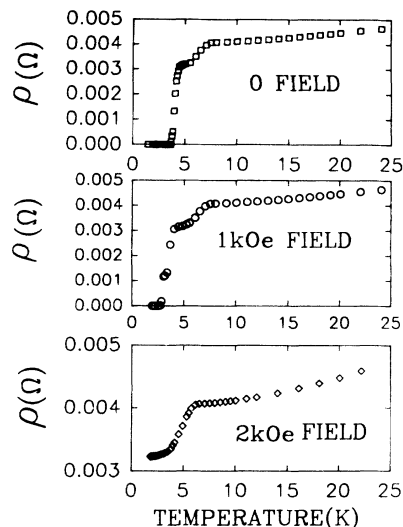


FIG. 13. Resistance of $\text{Sc}_{3.5}\text{Dy}_{1.5}\text{Ir}_4\text{Si}_{10}$ in dc magnetic fields.

perature dependence of χ from 60 to 300 K. The high temperature χ shows a Curie-Weiss behavior (similar to Dy-rich alloys) and an effective moment of $10.6\mu_B$. From the figure one can see that the sample undergoes superconducting transition before it becomes antiferromagnetic. The ac susceptibility in various dc magnetic fields clearly shows the antiferromagnetism as superconductivity is destroyed by the applied field. This data for two field values are shown in Fig. 12. We see that the sample has already become normal at an applied field of 2 KOe and above. The resistivity data shown in Fig. 13 show similar behavior at these fields. There is a small structure in the $\rho(T)$ near 4 K for low dc applied fields. The reason for such a structure is not clear and one has to wait for the single-crystal measurement to understand this behavior. The normal-state resistivity can be fitted to Eq. (2) and the data is shown in Fig. 14. The inset shows the superconducting transition of this sample.

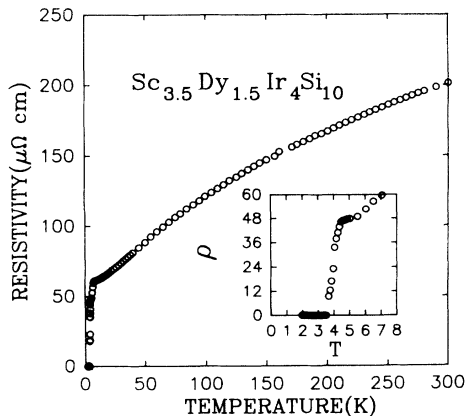


FIG. 14. Temperature dependence of resistivity of $\text{Sc}_{3.5}\text{Dy}_{1.5}\text{Ir}_4\text{Si}_{10}$. The inset shows the superconducting transition.

IV. CONCLUSION

We have studied the antiferromagnetism and superconductivity in $\text{Sc}_{5-x}\text{Dy}_x\text{Ir}_4\text{Si}_{10}$ ($x = 0, 0.5, 1, 1.5, 2, 3, 4, 4.5, 5$) system by using dc and ac susceptibility and resistivity measurements. The effective moment is equal to the free Dy ion for antiferromagnetic samples. The T_N

increases linearly with x (from $x = 2$) and T_C decreases somewhat rapidly as x increases to 1.5 and decreases below 1.5 K for $x = 2$ and above. The coexistence of superconductivity and magnetism is established for $x = 1.5$ using ac susceptibility and resistivity in small applied dc magnetic fields.

¹*Superconductivity in Ternary Compounds*, edited by M. B. Maple and Ø. Fisher (Springer-Verlag, Berlin, 1984), Vol. II.

²*Ternary Superconductors*, edited by G. Shernoy, R. Dunlap, and F. Fradin, (Elsevier—North-Holland, Amsterdam, 1981), p. 239.

³H. F. Braun and C. U. Sergè, *Solid State. Commun.* **35**, 735 (1980).

⁴S. Ramakrishnan, K. Ghosh, and Girish Candra, *Phys. Rev. B* **45**, 10 769 (1992).

⁵S. Ramakrishnan, R. S. Pandit, S. Sundram, and Girish Candra, *J. Phys. E* **18**, 650 (1985).

⁶See, for a review, S. K. Sinha, in *Handbook on the Physics and Chemistry of Rare Earths*, edited by K. A. Gschneidner, Jr. and L. Eyring (North-Holland, Amsterdam, 1978), Vol. 1, p.

489.

⁷R. J. Elliot and F. A. Wedgegood, *Proc. Phys. Soc.* **81**, 846 (1963).

⁸Review by S. Levgold, in *Magnetic Properties of Rare-Earth Metals*, edited by R. J. Elliot (Plenum, New York, 1972), p. 335.

⁹I. Das, E. V. Sampathkumaran, and R. Vijayaraghaven, *Phys. Rev. B* **44**, 159 (1991).

¹⁰L. S. Hausermann-Berg and R. N. Shelton, *Phys. Rev. B* **35**, 4673 (1987).

¹¹J. Pinski, P. B. Allen, and W. H. Butler, *Phys. Rev. B* **23**, 5080 (1981).

¹²L. S. Hausermann-Berg and R. N. Shelton, *Physica* **135B**, 400 (1985).